inter·noise 2021
1–5 August | Washington, DC

Thickness-resonance waves in underlays of floating screed

Charlotte Crispin[1]
Belgian Building Research Institute
Rue du Lombard 42, B-1000 Brussels, Belgium

Debby Wuyts[2]
Belgian Building Research Institute
Rue du Lombard 42, B-1000 Brussels, Belgium

Arne Dijckmans[3]
Belgian Building Research Institute
Rue du Lombard 42, B-1000 Brussels, Belgium

ABSTRACT

The prediction of the reduction of impact sound pressure level ΔL according to annex C of the standard ISO 12354-2 gives an acceptable estimation of the floating floor's performance for thin resilient layers. However, the performance is often largely overestimated for thick resilient layers or for resilient layers combined with thermal layers. One reason for this is that the simplified model doesn't account for the thickness resonances in the underlays which can greatly affect ΔL. This is confirmed by comparing finite element and transfer matrix method simulations with experimental results. This paper establishes the mechanisms leading to the development of these resonance waves and provides some guidelines to estimate their negative effects on the ΔL.

1. INTRODUCTION

In recent times, the thickness of thermal insulation layers under floating screeds has increased to meet more stringent energy performance requirements. Due to this increase in thickness, the resonance frequency of the first thickness-mode of this layer shifts down into the medium frequency range between 1000 and 5000 Hz depending on the thickness and type of the material. Thickness-modes are wave effects which occur when the thickness of the layer becomes comparable with multiples of the half-wavelength of the elastic waves traveling in the layers. These modes generate resonances that increase the vibratory transmission at specific frequencies.

A large number of laboratory tests have shown the negative impact of this thickness-mode on the improvement of impact sound insulation ΔL, as illustrated in Figure 1. It shows the ΔL measurement for a floating screed system composed of an acoustic and a thermal layer. This measurement result is compared to the classical constitutive model [1] based on force transmissibility theory, in which the floating floor system is considered as a linear damped single-degree of freedom sys-

[1] charlotte.crispin@bbri.be
[2] debby.wuyts@bbri.be
[3] arne.dijckmans@bbri.be

tem. While the simplified model generally gives good results for floating screed systems, it cannot accurately evaluate the actual acoustical behaviour of the floating floor with thermal layer above 315 Hz.

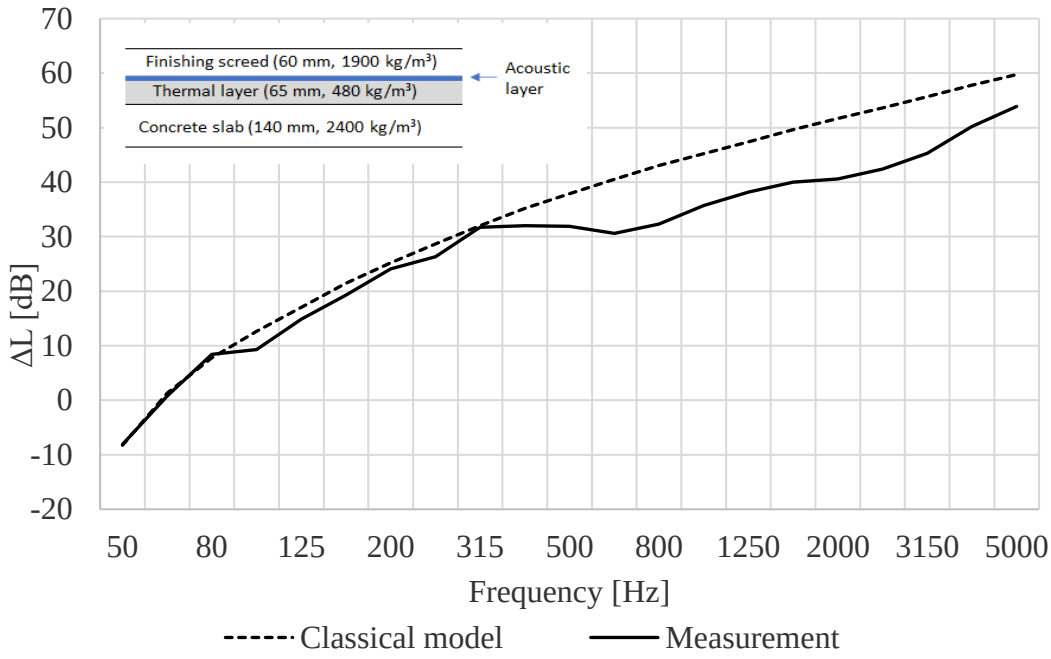

Figure 1: ΔL measured for a floating screed system on a supporting slab (140 mm, 2400 kg/m³) compared to the classical force transmissibility curve. The floating screed system consists of a cementitious screed (60 mm, 1900 kg/m³), an acoustic underlay (a felt, 7 mm, 49 kg/m³) and a thermal layer (65mm, 480 kg/m³).

Two floating screed systems, whose ΔL has been measured in the laboratory (EN ISO 10140-3:2021), are discussed below. These systems were used as a basis for the analysis of the problem and the comparison of predictive models.

The first case (CASE 1) studied is composed of a finishing screed (cement, 60 mm, 1900 kg/m³), a thermal layer (cement-based mortar with fine EPS beads, 65 mm, 125 kg/m³) and a slab (concrete, 140 mm, 2400 kg/m³). In the second case (CASE 2), an acoustic layer was added between the screed and the thermal layer (PE foam, 8mm, 25 kg/m³).

2. MEASUREMENT OF THE MECHANICAL PROPERTIES OF THE LAYERS

The knowledge of the mechanical properties of the different layers forming the two cases studied is important to understand the observed phenomena and as input data for the predictive models. The main mechanical properties (E, η) were measured with different experimental methods depending on the material and the frequencies of interest [2].

2.1. Properties of the acoustic resilient layer

The standard ISO 9052-1:1989 was used to determine the dynamic stiffness, s', of the acoustic resilient interlayer at low frequency. This measurement principle is based on the measurement of the mass-spring resonance frequency, fr, of a system composed of the sample loaded with a steel plate.

$$f_r = \frac{1}{2\pi}\sqrt{\frac{s'}{m''}} \text{ [Hz]} \quad (1)$$

Where s' is the dynamic stiffness of the sample [N/m³]

m" is the surface mass of the steel plate [kg/m²]

The Young's modulus, *E*, was then deduced with:

$$E = s'd \text{ [N/m²]} \tag{2}$$

Where d is the thickness of the sample [m].

The measurement of the bandwidth at half-power, Δf, of the resonant peak of this "mass-spring" system was also used to determine the damping, η, of the acoustic layer.

$$\eta = \frac{\Delta f}{f_r} \quad [-] \tag{3}$$

At high frequency, the Young's modulus of the acoustic resilient interlayer was deduced from the measurement of the first thickness resonance frequency of the sample, $f_{r,1}$ [1]. According to this method, the sample is placed between steel plates (Figure 2). A piezo-electrical transducer placed on top of the sample sends a white noise signal and the second transducer placed underneath the sample measures the frequency response function revealing the first thickness resonance:

$$f_{r,1} = \frac{c_L}{2d} \quad \text{[Hz]} \tag{4}$$

Where c_L is the velocity of the compressional wave [m/s].

And,
$$c_L = \sqrt{\frac{E}{\rho}} \tag{5}$$

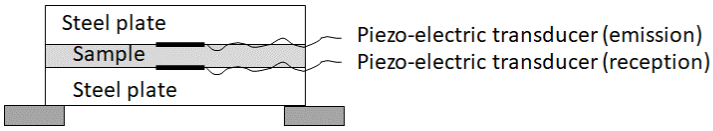

Figure 2: Setup for the measurement of the first thickness resonance frequency of an acoustic layer

2.2. Properties of the solid layers (screed, thermal layers and slab)

At low frequencies, an equivalent complex Young's modulus, *E*, of the thermal layer was determined by fitting the measured first bending mode dispersion curve with a finite element model. The measurements were carried out on a sample with a size of 400 mm x 400 mm that is excited at its center with a shaker.

At high frequencies, the Young's modulus, *E*, of the three solid layers was determined by the measurement of the quasi-longitudinal phase velocity. For this measurement, two accelerometers, separated by a distance d, were used to detect the arrival time of the quasi-longitudinal wave generated by a hammer hit. The quasi-longitudinal wave velocity and Young's modulus are then calculated from [3]:

$$c_L = \frac{d}{\Delta t} \tag{6}$$

$$E = c_L^2 * \rho(1 - \nu^2) \tag{7}$$

Where ρ is the density [kg/m³] and ν the Poisson coefficient [-] of the thermal layer, assumed to be 0.2.

The total loss factors of the screed and the concrete slab were determined by the measurement of the structural reverberation times, T_s. The impact hammer was used as method of excitation. The relation between the total loss factor η and the structural reverberation time T_s is given by:

$$\eta = \frac{2.2}{fT_s} \tag{8}$$

The damping of the thermal layer could not be measured because it was not accessible.

2.3. Measurement results

Table 1 : Measurement results of the mechanical properties of the different layers

	Concrete slab	**Thermal layer**	**Acoustic layer (PE foam)**	**Finishing screed**
Thickness [mm]	140	65	8	60
Density [kg/m³]	2400	125	25	1900
E [Pa] at low frequencies	-	4.05e+7	1.5e+05	-
η [-] at low frequencies	0.06	-	0.3	0.04
E [Pa] at high frequencies	2.2e+10	2.83e+7	8.50E+04	1.74e+10
η [-] at high frequencies	0.01	-	-	0.02

3. ANALYTICAL MODELS

Theoretical studies of thickness resonances in isolation mounts have been made by several authors [4, 5]. They have developed analytical models of transmissibility that take into account these standing waves. Because similar phenomena are involved, the measurement results of ΔL are compared with the analytical model of Harrison.

$$|T^2| = \frac{1+5n^2}{\left[\begin{array}{c}\left(1+5n^2+\left(\frac{\omega}{\omega_0}\left(\frac{M}{m}\right)^{\frac{1}{2}}\right)^2\right)sinh^2\left(n\frac{\omega}{\omega_0}\left(\frac{M}{m}\right)^{\frac{1}{2}}\right)+n\frac{\omega}{\omega_0}\left(\frac{M}{m}\right)^{\frac{1}{2}}sinh\left(2n\frac{\omega}{\omega_0}\left(\frac{M}{m}\right)^{\frac{1}{2}}\right)\\ +(1+5n^2)cos^2\left(\frac{\omega}{\omega_0}\left(\frac{M}{m}\right)^{1/2}\right)+\left(\frac{\omega}{\omega_0}\left(\frac{M}{m}\right)^{1/2}\right)^2 sin^2\left(\frac{\omega}{\omega_0}\left(\frac{M}{m}\right)^{1/2}\right)-\frac{\omega}{\omega_0}\left(\frac{M}{m}\right)^{\frac{1}{2}}(1+n^2)sin\left(2\frac{\omega}{\omega_0}\left(\frac{M}{m}\right)^{1/2}\right)\end{array}\right]} \tag{9}$$

And, $$\Delta L_{Harrison} = 20\lg\left(\left|\frac{1}{T}\right|\right) \quad \text{[dB]} \tag{10}$$

Where n is the damping ratio of the thermal layer ($n \approx \eta/2$)
M is the surface mass of the screed [kg/m²]
m is the surface mass of the thermal layer [kg/m²]

And, $$\omega_0 = \left(\frac{s\prime}{M}\right)^{1/2} \tag{11}$$

The standing wave resonant frequencies are given by:

$$\omega_i = \omega_0 i\pi\left(\frac{M}{m}\right)^{1/2} \qquad \text{i=1,2,3,…} \tag{12}$$

The measurement results of ΔL are also compared with the classical theory [1].

$$\Delta L_{classical} = -20lg\left[\sqrt{\frac{1+\eta^2\left(\frac{f}{f_0}\right)^2}{\eta^2\left(\frac{f}{f_0}\right)^2+\left(1-\frac{f^2}{f_0^2}\right)}}\right] \text{[dB]} \quad (13)$$

3.1. CASE 1: Thermal layer without acoustic interlayer

For case 1, the best fit of Harrison's model is obtained with half the measured Young's modulus at low frequency (Table 2). The resonance dip of the mass-spring system around 250 Hz is overestimated by both analytical models (Figure 3).
The resonance frequency f1 of the 1st thickness-mode is relatively well estimated by Harrison's model. At these high frequencies, the measured Young's modulus is 1.4 times greater than the modulus used for the fit. While Harrison's model predicts a sharp dip around f1, the resonance dip in the measurement is much broader, which can be explained by various reasons.

- The thickness of the thermal layer varies with ± 1.5 cm over the entire test surface;
- The Young's modulus depends on the frequency. When the wavelength becomes an appreciable fraction of the thickness of the layer, the compressional wave velocity is lower than the value given by $c_L=(E/\rho)^{1/2}$. This decrease in the velocity is caused by the radial motion [4]. This difference is also observed in the Young's modulus measurement results.
- The damping could be underestimated.

Table 2 : Mechanical properties used to model CASE 1

	Thermal layer	**Finishing screed**
Thickness [mm]	65	60
Density [kg/m³]	125	1900
E [Pa]	1.97e+7	-
η [-]	0.3	-

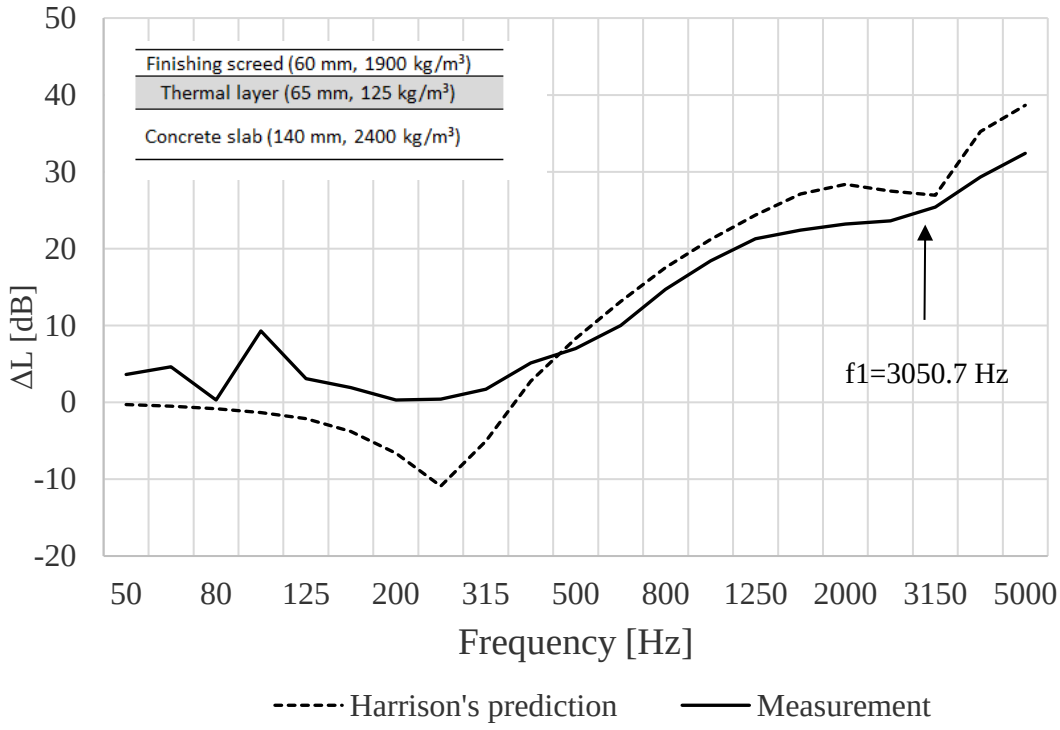

Figure 3: Case 1 (thermal layer without acoustic interlayer): measurement versus analytical models

3.2. CASE 2: Thermal layer with acoustic interlayer

The theoretical model of Harrison does not currently allow calculations for a thermal layer combined with an acoustic layer. In order to apply the theoretical model, it is necessary to define an equivalent layer that takes into account the mechanical properties of both layers. Therefore, the mass-spring resonance frequency ω_0 of Equation 11 must take into account the dynamic stiffnesses of the two layers:

$$\omega_0 = \sqrt{\frac{s'_{eq}}{M}} \text{ [Hz]} \tag{14}$$

Where

$$s'_{eq} = \frac{s'_{Th}\, s'_{Ac}}{(s'_{Th} + s'_{Ac})} \tag{15}$$

And s'_{Th} is the dynamic stiffness of the thermal layer [N/m³];
s'_{Ac} is the dynamic stiffness of the acoustic interlayer [N/m³];

For case 2, the best fit of Harrison's model to the measured results is obtained with the mechanical properties for the equivalent layer given in Table 3, these values are obtained with Equation 14 using a Young's modulus of 4.05e+7 Pa for the thermal layer and a Young's modulus of 1.8+05 Pa for the acoustic layer:

Table 3 : Mechanical properties used to model CASE 2 with an equivalent layer

	Equivalent layer	**Finishing screed**
Thickness [mm]	73	60
Density [kg/m³]	114	1900
E [Pa]	2.09e+6	-
η [-]	0.3	-

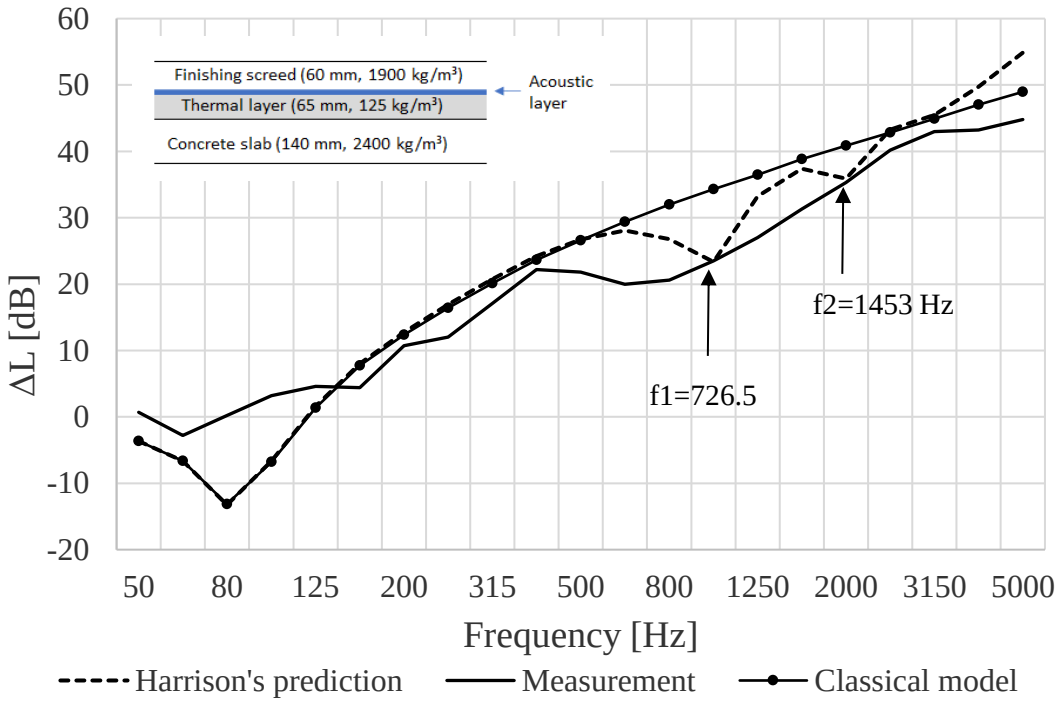

Figure 4: Case 2 (thermal layer with acoustic interlayer): measurement versus analytical models

The thickness resonance frequencies are slightly overestimated by the adjusted model of Harrison compared to the measurement results (Figure 4). A better fit would be obtained with a lower Young's modulus at high frequencies.
It could of course be expected that the theoretical model cannot be applied to systems composed of two different underlayers since at high frequencies, standing waves occur in each layer independently. These standing waves should be independent of the resonant frequency of the combined mass-spring system. Indeed, Harrison shows that the velocity V1, which determines the resonant frequency of the first standing wave, is the average velocity through both layers.

$$V_1 = \frac{2}{\rho^{1/2}} \frac{(E_{Th} E_{Ac})^{1/2}}{E_{Th}^{1/2} + E_{Ac}^{1/2}} \tag{16}$$

This means that the Young's modulus determined from Equations 14, 15 and 2 gives an overestimation at high frequencies.
Unfortunately, in Harrison's model, the transmissibility and the standing wave frequencies are calculated based on a constant Young's modulus. Furthermore, the thickness-resonance frequencies are calculated from the mass-spring resonance frequency according to Equation 12 which does not currently allow calculations with a Young's modulus depending on the frequency.

4. FEM AND TMM MODELS

To overcome the limitations of the analytical models, finite element (FEM) and transfer matrix (TMM) models are used that allow to estimate the ΔL taking into account mechanical properties that depend on the frequency.

For the FEM calculations, the commercial software Actran (Version 15.1) was used. The isotropic solid elements with KRYLOV with MUMPS solver were chosen. The models represent the measured complexes in real size (4.1 m x 2.6 m). The mesh size was chosen in order to be six times finer than the first thickness-mode wavelength. For the boundary condition, a simple support was modelled by restraining the transverse translational degree of freedom of the boundary of the lower surface. The frequency range covered one-third octave bands between 50 Hz and 5000 Hz using a logarithmic increment. Results were calculated and averaged at five or six frequencies in each one-third octave band. Excitation of the source plate was applied using three non-correlated point forces. The spatial-average velocity level was calculated on the concrete slab using the radiating surface which can give the normal mean square velocity of this surface. The ΔL is obtained by taking the difference between the normal mean square velocity of the bare slab and the normal mean square velocity of the slab bearing the floating screed.

For the TMM calculations, the MATLAB application WinLayers [2] was used. One of the main assumptions in the TMM is plane wave propagation through the multi-layered structure. To model the impact sound insulation of a point force excited structure in the TMM, the sound field is decomposed into plane wave components. The ΔL is calculated from the resulting sound pressure levels beneath the point-excited floors with and without floating screed. Results were calculated for infinite structures at 9 frequencies per one-third octave band and averaged. Diffraction effects caused by the finite dimensions of the floors can be taken into account by a spatial windowing technique. Because the diffraction only depends on the size of the structure, the ΔL-prediction is however independent of the floor size.

For the FEM and TMM models, a linear decay with frequency was applied to the Young's modulus of the thermal layer. A Poisson's ratio of 0.2 was chosen for the three solid materials.

Table 5 : Mechanical properties used in FEM and TMM

	Concrete slab	Thermal layer	Acoustic layer	Finishing screed
Thickness [mm]	140	65	8	60
Density [kg/m³]	2445	125	25	1900
E [Pa] at 50 Hz	2.2e+10	1.97e+7	2.4e+5	1.74e+10
η [-]at 50 Hz	0.06	0.8	0.2	0.04
E [Pa] at 5000Hz	2.2e+10	1.64e+7	2.4e+5	1.74e+10
η [-]at 5000Hz	0.01	0.1	0.1	0.02

4.1. CASE 1: Thermal layer without acoustic interlayer

At low frequencies, where the same Young's modulus was used as for Harrison's analytical model, the FEM and TMM models slightly overestimate the resonance frequency of the mass-spring system compared to the one observed in the measurement results (315 Hz instead of 250 Hz) (Figure 5). This discrepancy could be partly explained by a poor estimation of the Poisson's ratio, which plays a non-negligible role in the determination of this resonance.
In the models, the first standing wave resonance dip is clearly visible at around 3150 Hz. Both FEM and TMM overestimate ΔL around 1850 Hz at which an anti-resonance is predicted, but this peak is not visible in the measurement results. As explained in section 4.1, the resonance dip in the measurement result is spread out due to the variability of the thermal layer thickness and probably a more pronounced Young's modulus decay when the wavelength becomes an appreciable fraction of the thickness of the layer. This may also explain why the anti-resonance peak is not visible in the measurements.

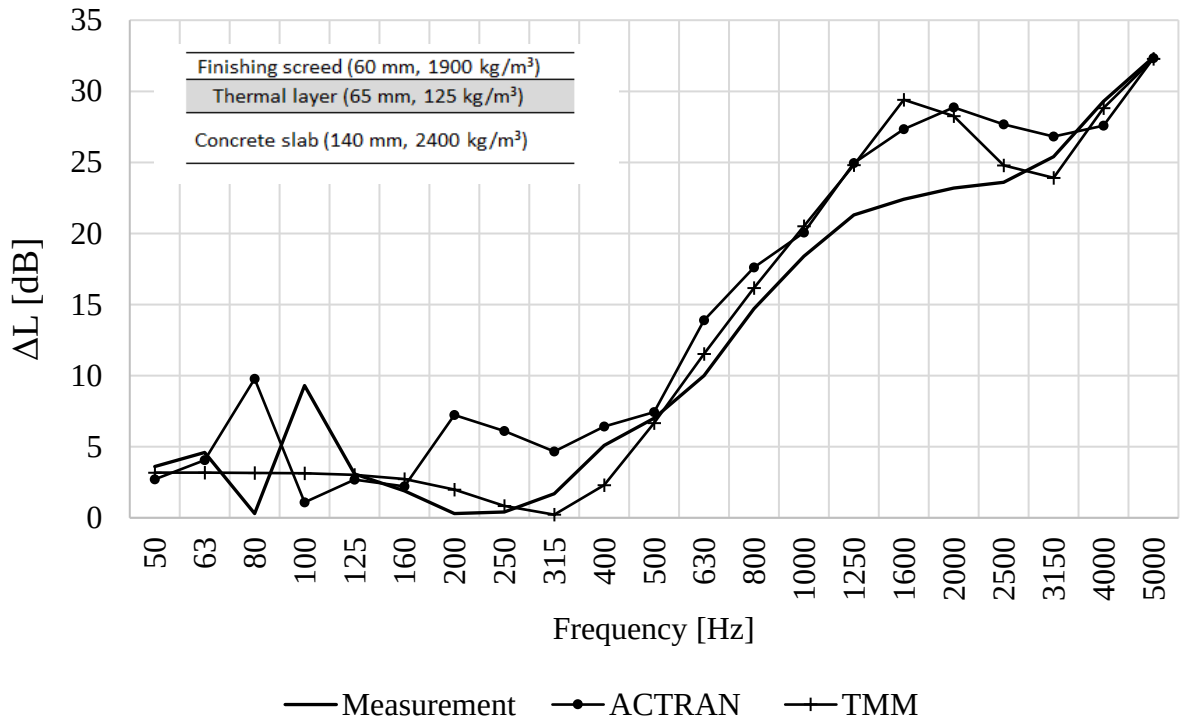

Figure 5: Case 1 (thermal layer without acoustical interlayer): measurement versus FEM and TMM

4.2. CASE 2: Thermal layer with acoustic interlayer

For case 2, the FEM and TMM predictions don't match the measurements when the thermal and acoustic layer are modelled as two separate, perfectly bonded elastic layers with the properties of

Table 5 (figure 6, ACTRAN and TMM). The use of an equivalent layer having mechanical properties equivalent to the two combined layers gives a better agreement (figure 6, ACTRAN (equivalent layer) and TMM (equivalent layer)). It seems that the bond between the different layers plays an important role. Near the contact surface, where the thermal layer is bonded to the relatively stiff concrete screed (or the relatively soft acoustic layer), the effective modulus of the material increases (or decreases), resulting in an increase (or decrease) in effective modulus. This phenomenon which is called the "end effect" does not seem to be well managed by the FEM or TMM calculations. In his article, Harrison has shown the influence of this "end effect". The variability of the ratio ω1/ ω0 between different combinations of layers could be a consequence of this "end effect" having a different influence upon the low resonant frequency and the standing wave frequencies.

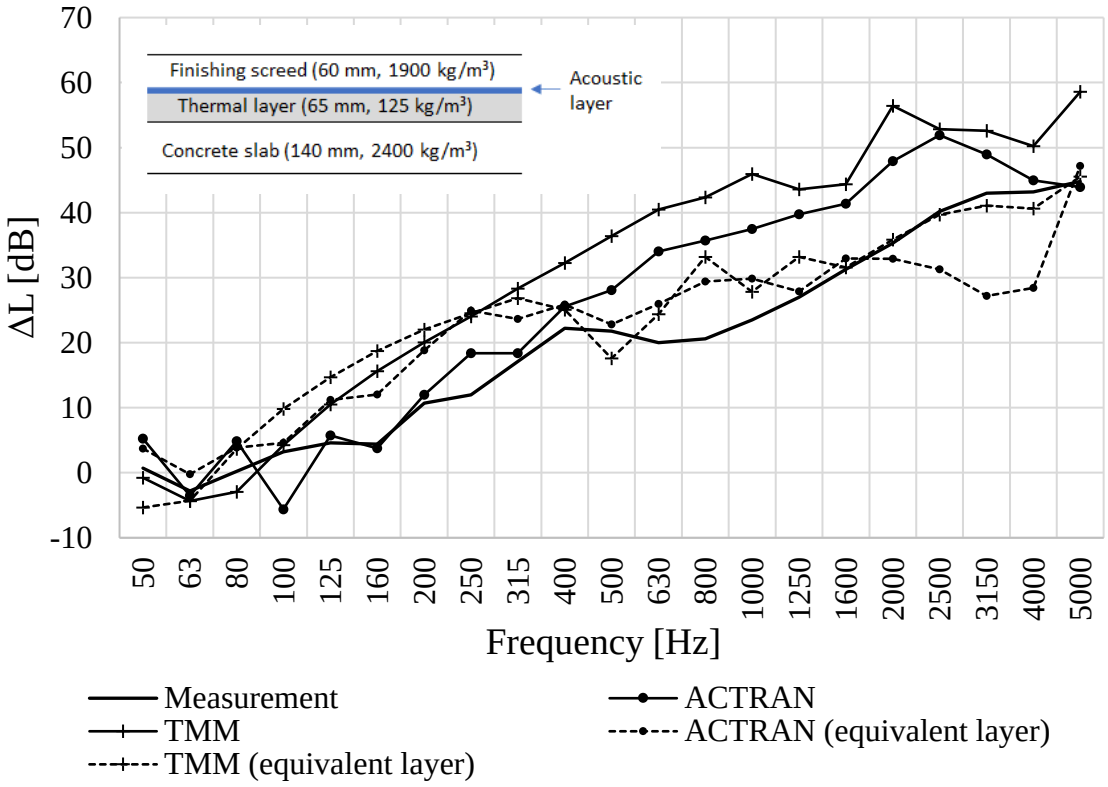

Figure 6: Case 2 (thermal layer with acoustical interlayer): measurement versus FEM and TMM

5. DISCUSSION OF RESULTS

The manifestation of standing waves will occur at lower frequencies the higher the density and thickness of the thermal layer and the lower the Young's modulus of this layer. As we have seen before, the bonding of a thermal layer with an acoustic layer will also have the effect of lowering the frequency of the first standing wave by the "end effect".

The damping of the thermal layer has a significant influence (Figure 7). The measurement results are obtained for combinations consisting of the same acoustic interlayer but with a thermal layer that differs only by its damping.
A low damping of the thermal layer accentuates the resonance dips caused by the standing waves and results in a lower ΔL than predicted by the classical model (Figure 7a). Conversely, high damping reduces the effect of resonance. At high frequencies, the dissipative effect in the medium in which the elastic waves propagate even causes an exponential increase in ΔL which is not taken into account by the classical model (Figure 7b).

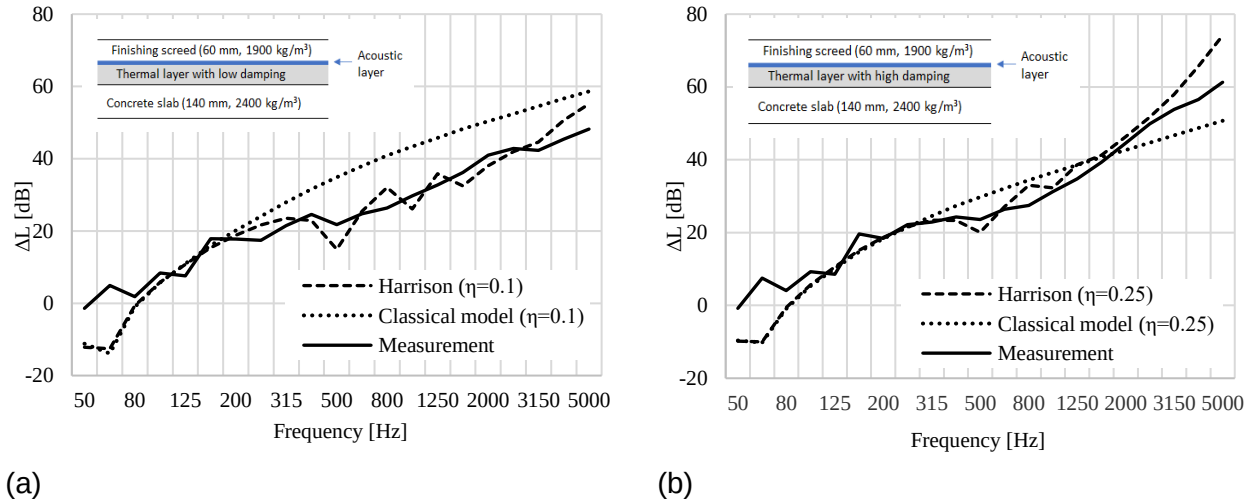

(a) (b)

Figures 7: Comparison of measured ΔL with the analytical models for two different thermal layer compositions - a) for a thermal layer with low damping - b) for a thermal layer with high damping.

Figures 8 illustrates the effect of the thickness of a thermal layer on ΔL. Figure 8a presents the measured ΔL for two complexes: a complex consisting of a 15 mm thermal layer and a complex consisting of the same thermal layer but with a thickness of 60 mm. As expected, the resonance frequency of the mass-spring system of the thicker thermal layer system is lower: it is at 200 Hz while that of the thinner complex is at 250 Hz. From this resonance frequency, and according to the classical model, the ΔL of the thicker complex should have higher values, but the appearance of the standing waves (f1,60 mm at 630 Hz and f2,60 mm at 1250 Hz) causes a drop in the ΔL, which then joins the curve of the thinner complex. At high frequencies, the thick layer regains the advantage thanks to its higher damping.

Figures 8b presents the Harrison's models for these cases. The predictions confirm the observations from the measurement results. The frequencies of the standing waves are well identified but the dips are more pronounced compared to measurement results due to an underestimation of the damping.

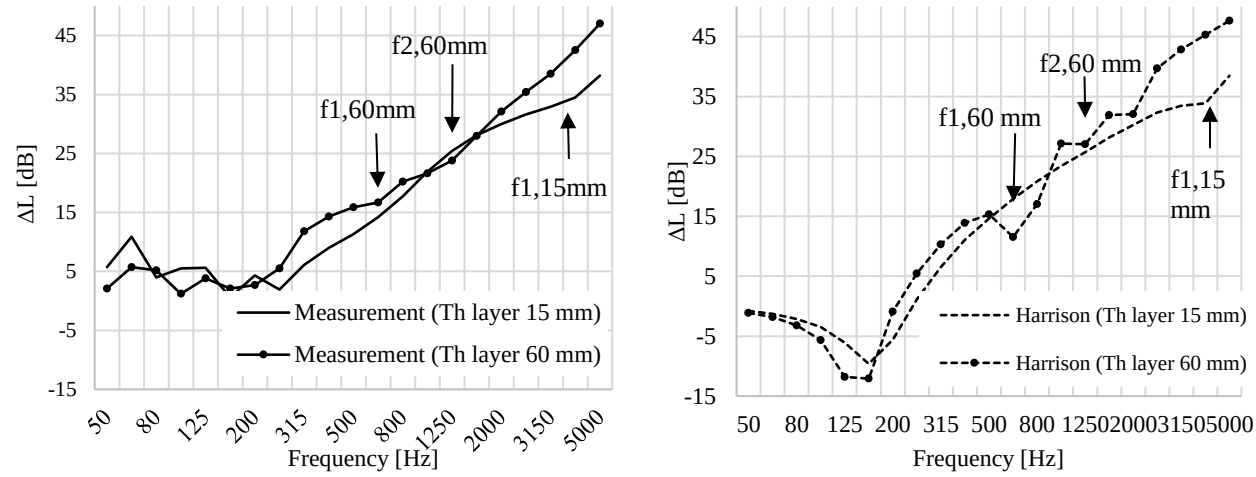

(a) (b)

Figures 8: Analysis of the effect of thermal layer thickness on ΔL -a) from measured results – b) from the Harrison's prediction.

6. CONCLUSIONS

In recent times, the thickness of thermal insulation layers under floating screeds has increased to meet more stringent energy performance requirements. This increase in thickness has caused the appearance of thickness resonances into the medium frequency making the classical constitutive model based on force transmissibility theory inaccurate to evaluate the actual acoustical behaviour of a floating floor in the medium and high frequency ranges.

The Harrison's analytical model was used to study the influence of these standing waves on ΔL. This model has been shown to be quite effective in locating the thickness resonance frequencies for a single layer complex. This model showed the positive impact of a high damping of the thermal layer due to the dissipation of elastic waves in the medium. It also showed that a thicker thermal layer offered no (or little) improvement in the mid-frequency range on ΔL compared to a thin layer. However, this analytical calculation should be taken with caution as it does not allow for the modelling of a frequency-dependent Young's modulus. Indeed, it has been shown that when the wavelength becomes an appreciable fraction of the thickness of the layer, radial motion leads to a decrease in wave velocity.

When a complex is composed of two layers (thermal layer combined with an acoustic layer), Harrison's model requires the definition of an equivalent layer. In this case, the thickness resonance frequencies are overestimated compared to those measured. This is due to the fact that the model does not take into account the radial motion but also the "end effect", the increase of the damping with increasing frequency and the decrease of the compression wave velocity for the waves which travel through the two different materials.

The FEM and TMM models were then applied in order to take into account a Young's modulus decreasing with increasing frequency. These models offer satisfactory results for single layer complexes. The results of the calculations for "double layer" complexes are not satisfactory and do not allow to highlight the decrease of the compression wave velocity. This would argue in favour of an "end effect" since it is not well managed by these models.

7. REFERENCES

1. Schiavi, A. Improvement of impact sound insulation: A constitutive model for floating floors. *Applied Acoustics,* **129**, 64-71 (2018).
2. Geebelen, N. Structure-borne sound sensitivity of building structures. Assessment of the acoustic performances of multi-layered structures by simulation and measurement techniques. *PhD thesis*, Katholieke Universiteit Leuven (2008).
3. Hopkins, C. Sound Insulation, *Elsevier* (2007).
4. Harrison, M, Sykes, A.O., Martin M. Wave effects in isolation mounts*, Report 766, Navy Department*, Washington (revised edition 1964).
5. Snowdon, J.C. Vibration and shock in damped mechanical systems, *John Wiley and Sons* (1968).